Journal of Catalysis **193,** 108–114 (2000)
doi:10.1006/jcat.2000.2868, available online at http://www.idealibrary.com on IDEAL®

Pd Segregation to the Surface of Bimetallic Pt–Pd Particles Supported on H-β Zeolite Evidenced with X-Ray Photoelectron Spectroscopy and Argon Cation Bombardment

Lucien Fiermans,* Roger De Gryse,* Geert De Doncker,* Pierre A. Jacobs,† and Johan A. Martens†,[1]

*Vakgroep Vaste-stofwetenschappen, Universiteit Gent, Krijgslaan 281/S1, B-9000 Gent, Belgium; and †Centrum voor Oppervlaktechemie en Katalyse, K.U. Leuven, Kardinaal Mercierlaan 92, B-3001 Heverlee, Belgium

Received December 17, 1999; revised March 9, 2000; accepted March 9, 2000

Bimetallic PtPd/H-β hydrocracking catalyst samples with 1.75 and 3.5 wt% metals, Pt : Pd atomic ratio of 3 : 1, and metal particle size of 1.7 nm were prepared using impregnation and cation exchange of Pt^{2+} and Pd^{2+} tetrammine complexes, oxidation, and hydrogen reduction at 400°C. The dispersed metal phases were characterized using XPS. The formation of bimetallic Pt–Pd particles with segregation of the palladium to the particles surfaces was evidenced by intensity changes of the Pd 3*d* and Pt 4*d* photolines upon bombardment with argon cations and by comparison with a physical mixture of monometallic Pd/H-β and Pt/H-β catalysts, subjected to the same treatment.

Key Words: **hydrocracking catalyst; bimetallic; platinum; palladium; β zeolite; X-ray photoelectron spectroscopy; argon bombardment; surface segregation.**

INTRODUCTION

There are many examples of multimetallic catalysts in which the association of two or more metals has a beneficial influence on catalyst properties such as activity, selectivity, and deactivation by coke deposition and sulfur poisoning (1). The combination of platinum and palladium is particularly advantageous in catalysts for hydroisomerization, hydrocracking, hydrogenation, and hydrotreatment. For example, a bimetallic catalyst containing platinum and palladium metals on alumina has improved sulfur resistance in a diesel hydrotreating process compared to a platinum monometallic catalyst (2). Pt–Pd combinations supported on amorphous silica–alumina are superior catalysts for second-stage deep hydrodesulfurization and show enhanced hydrogenation activity (3). β zeolites loaded with platinum and palladium metals (PtPd/H-β) have a higher sulfur tolerance in hexane hydroisomerization compared to monometallic Pt/H-β and Pd/H-β catalysts (4). The improved sulfur resistance was proposed to result from a decreased electron density on the platinum in the presence of palladium (2, 4). Palladium was also inferred to inhibit the sintering of a dispersed platinum phase (2, 3). Pt/H-β is an excellent hydroisomerization catalyst for short *n*-alkanes in the absence of sulfur (5–9). Substitution of a fraction of the platinum metal of a Pt/H-β catalyst with palladium improves the catalytic activity and the isomerization selectivity of heptane (9). The combination of the two metals in the PtPd/H-β catalysts gives rise to a better noble metal dispersion in comparison to the monometallic catalysts (9). It leads to a better proximity of the metal and the acid sites and a better balance of the metal and acid catalytic functions (9). A key question that remains to be addressed is the nature of the noble metal particles in PdPt/H-β zeolites.

Platinum–palladium alloy formation was observed on low surface area aluminosilicate supports (10, 11). Pumice-supported Pd–Pt bimetallic catalysts with metal particle sizes between 2.5 and 5.3 nm, depending on the noble metal composition and preparation at low temperature using metal allyl complexes, were characterized using WAXS, SAXS, and XPS (11, 12). The presence of an alloy was deduced from the shifting of the [111] reflection upon hydrogen adsorption, monitored with WAXS (11). The less abundant metal was segregated to the surface of these alloy particles, as derived from the Pd/Pt ratio at the surface, determined with XPS, to the bulk composition and from the dependence of the Pd 3*d*/Pd MNN intensity ratio on the Pd/Pt composition (12).

Compared to supports with low specific surface area, the characterization of the Pd–Pt metal phases in zeolite catalysts is more difficult given the microporous nature of the zeolite support and the typically low metal loading. Rades *et al.* prepared PtPd/Na-Y zeolites with high metal loading using cation exchange with $Pd(NH_3)_4^{2+}$ and $Pt(NH_3)_4^{2+}$, calcination, and hydrogen reduction at 300°C and characterized the metals with TEM, TPR, and EXAFS (13). In these samples containing from 6 to 10.5 wt% metals and Pt : Pd atomic ratios of 3 : 1, 1 : 1, and 1 : 3, the existence of bimetallic particles with diameters from 1.5 to 1.9 nm

[1] Corresponding author. Fax: +32 16 321998. E-mail: johan.martens@agr.kuleuven.ac.be.

0021-9517/00 $35.00

increasing with the Pd content was derived from the EXAFS. With increasing Pt content, the cluster core became richer in platinum and the surface richer in palladium. Hansen *et al.* studied hydrogen dealuminated Y zeolite containing a substantial amount of extra-framework aluminum with a Pd–Pt metal loading of about 2 wt% and Pt : Pd atomic ratio in the range from 1 : 1 to 1 : 3 prepared using incipient wetness impregnation with solutions of metal tetraamine complexes and calcination and reduction at 300°C (14). In those PtPd/H-Y zeolites with the average metal particle size increasing from 1.5 nm for the pure Pt sample to 3.1 nm for the pure Pd end member, the EXAFS provided evidence for segregation of palladium to the surface of the metal particles. From the results of TPR, hydrogen TPD, hydrogen chemisorption, and FT-IR spectroscopy of adsorbed carbon monoxide, Lee and Rhee postulated Pd–Pt alloy formation in their PtPd/H-β samples prepared by impregnation of the zeolite with noble metal tetraamine complexes, calcination at 350°C, and hydrogen reduction at 500°C (4).

In conclusion, platinum and palladium form nanometer-sized bimetallic particles on various supports. In Pt–Pd bimetallic particles supported on zeolites and prepared using metal tetraamine complexes and calcination and reduction at elevated temperatures, there is evidence for Pd segregation to the surface of the metal clusters. In this work, we used XPS and argon ion bombardment to characterize a bimetallic PtPd/H-β sample, the hydrocracking performances of which were reported earlier (9). A comparison with physical mixtures of monometallic Pt/H-β and Pd/H-β catalysts was used to probe surface enrichment.

EXPERIMENTAL

An overview of the catalyst samples is given in Table 1. The H-β zeolite sample was a commercial product (CP 811 from PQ, type 304). NH_4-β was obtained by slurrying the H-β powder in a diluted aqueous solution of NH_4OH at room temperature. Metal-loaded samples were prepared as follows. 3.0Pt0.5Pd/H-β and 0.25Pd/H-β samples were prepared by impregnating H-β dried in air at 60°C according to the incipient wetness technique with the appropriate amount of aqueous solution of $Pt(NH_3)_4Cl_2$ and/or $Pd(NH_3)_4Cl_2$ to obtain the indicated Pt and Pd loading expressed in wt%. 1.5Pt/H-β was obtained by slurrying NH_4-β in the appropriate amount of 1 mmol/L aqueous solution of $Pt(NH_3)_4Cl_2$. 1.5Pt0.25Pd/H-β was prepared in the same way using a solution containing $Pd(NH_3)_4Cl_2$ in addition to $Pt(NH_3)_4Cl_2$. After the ion exchange, the zeolite powder was recovered by filtration, washed on the filter until no chlorine was left in the wash water, and dried.

One gram of dry sample, compressed into particles with diameters from 0.25 to 0.5 mm, was loaded in a quartz tube and heated in flowing oxygen (20 ml/min) to 400°C at 5°C/min. After 1 h, the sample was purged with nitrogen and subsequently reduced in flowing hydrogen at the same temperature without intermittent cooling.

The physical mixture of 1.5Pt/H-β and 0.25Pd/H-β was obtained by mixing equal weights of the two reduced powders in a mortar.

Noble metal dispersions were previously determined using hydrogen chemisorption and TEM (8, 9). The platinum dispersion in the 1.5Pt/H-β sample was 41%, corresponding to a particle size of 2.5 nm (8). This particle size was confirmed with TEM, showing an additional very small number of larger particles with diameters up to 10 nm (8). The metal dispersion of 0.25Pd/H-β could not be reliably determined due to the low metal content. Similar samples with a Pd content of 1 wt% have a low dispersion of around 8%. The two bimetallic catalysts, independent of metal loading and preparation technique, have a metal dispersion of ca. 60%, corresponding to a metal particle size of ca. 1.7 nm (9).

Before the XPS spectra were recorded, the powder samples compressed into pellets in ambient air were subjected to a supplementary hydrogen reduction treatment at 300°C and passivated with carbon dioxide. The pellet was rapidly transferred into the XPS apparatus to minimize exposure to ambient air.

The XPS spectra were recorded with a Perkin-Elmer PHI 5500 ESCA system, using monochromated Al$K\alpha$ radiation (1486.6 eV). The samples were evacuated in high vacuum (10^{-6} Pa) for 24 h before the spectra were recorded. Argon

TABLE 1

Catalyst Samples

	3.0Pt0.5Pd/H-β	1.5Pt0.25Pd/H-β	1.5Pt/H-β	0.25Pd/H-β	1.5Pt/H-β + 0.25Pd/H-β physical mixture
Pt content (wt%)	3.0	1.5	1.5	—	0.75
Pd content (wt%)	0.5	0.25	—	0.25	0.125
Zeolite particle size (μm)	0.1–0.7	0.1–0.7	0.1–0.7	0.1–0.7	0.1–0.7
Metal particle size (nm)	1.7	1.7	2.5	N.D.[a]	—

[a] Not determined, metal loading too low for accurate determination; a 1Pd/H-β sample prepered in the same way has a Pd particle size of 13 nm.

TABLE 2

Binding Energies

	Before sputtering			After sputtering		
	3.0Pt0.5Pd/H-β	1.5Pt0.25Pd/H-β	1.5Pt/H-β + 0.25Pd/H-β physical mixture	3.0Pt0.5Pd/H-β	1.5Pt0.25Pd/H-β	1.5Pt/H-β + 0.25Pd/H-β physical mixture
Pd 3*d*5	335.4	335.4	335.4	335.9	335.8	336.6
Pd 3*d*3	340.7	340.7	340.7	341.1	341.1	341.9
PdOx 3*d*5	338.0	338.0	338.0	336.9	338.4	339.2
PdOx 3*d*3	343.3	343.3	343.3	342.1	343.7	344.5
Pt 4*d*5	314.3	314.5	314.5	314.9	315.1	315.2
Pt 4*d*3	331.3	331.5	331.5	331.9	332.1	332.2
PtOx 4*d*5	317.0	318.0	318.0	317.5	317.8	317.9
PtOx 4*d*3	334.0	335.0	335.0	334.5	334.8	334.9
Pt 4*f*7	71.4	71.2	71.1	72.2	71.4	71.6
Pt 4*f*5	74.8	74.6	74.5	75.6	74.8	75.0
PtOx 4*f*7	74.1	74.7	74.6	74.9	74.1	74.3
PtOx 4*f*5	77.4	78.0	77.9	78.2	77.4	77.6
CaOx 2*p*3	347.9	347.9	347.7	347.4	347.3	348.4
CaOx 2*p*1	351.4	351.4	351.2	350.9	350.8	352.9
Al 2*p*				73.4	72.5	73.0
AlOx 2*p*1	74.8	73.9	74.1	75.3	74.4	74.9
Ar 2*s*				319.7	318.8	319.2
C 1*s*	284.3	284.3	284.3	284.3	284.3	284.3

cations were used for ion bombardment at 2.5 kV on an area of 2.5×2.5 mm. The Ar^+-ion bombardment was applied for 2 h.

The XPS spectra exhibited only very weak Pd 3*d* and Pt 4*d* signals. These XPS photolines were superimposed on the plasmon losses of the unavoidable strong C 1*s* peak. The Pt 4*f* photolines coincide with the Al 2*p* peak and were not readily interpretable. Therefore, background subtraction and curve-fitting procedures were applied to all spectra. In the Pd 3*d* and Pt 4*d* range the plasmon peaks were subtracted by superimposing and scaling the plasmon spectrum of the C 1*s* line on the spectra. To this purpose, the Si 2*s* plasmon spectrum was used because this spectrum could be recorded in an otherwise unperturbed energy range. It was assumed that the plasmon structure determined by the bulk was identical at the C 1*s* and Si 2*s* photolines. Next to the plasmons, a standard background subtraction procedure, well known in the XPS field as the Shirley procedure, was applied. After these subtraction procedures, the experimental curve in the Pd 3*d*, Pt 4*d* range was fitted with Gaussian–Lorentzian (80%–20%) line shapes at the well-established Pd $3d_{5/2}$ and Pd $3d_{3/2}$, Pt $4d_{5/2}$, and Pt $4d_{3/2}$ peak positions (Table 2). In the fitting procedure, peaks of electron-deficient Pt and Pd were introduced at fixed binding energy values for PdO and/or PdO_2 and PtO and/or PtO_2 taken from the literature (16). For each metal, the oxide peak positions giving the best agreement were used in the fitting.

In the Pt 4*f*, Al 2*p* region, a general Shirley background subtraction was applied together with curve fitting for the Pt $4f_{7/2}$, Pt $4f_{5/2}$, and Al 2*p* photolines. It is our experience that some oxides such as Al_2O_3 and TiO_2 exhibit reduction upon bombardment with Ar^+, resulting in the formation of metallic Al and Ti, respectively, ascribed to preferential sputtering of oxygen. In our curve fitting of Ar-bombarded samples, we added a small peak at the position for Al in the metallic state.

The same procedures were applied to the spectra before and after Ar^+ bombardment. Pt : Pd and Al : Pt concentration ratios were calculated with the appropriate areas of the corresponding metal and oxide peaks and with use of the established sensitivity factors. The error on the atomic ratios derived from the spectra was estimated at ±20%.

In all samples, and especially in 3.0Pt0.5Pd/H-β, unexpectedly strong Ca 2*p* lines were detected. The Ca/Al concentration ratio on the surface of the crystals derived from the XPS signal intensities was 0.12, decreasing after Ar^+ bombardment. Calcium appeared to be an impurity in this commercial zeolite β sample.

In two additional XPS experiments, the Pd $3d_{5/2}$/Pd(MNN) intensity ratio was determined on the 3.0Pt0.5Pd/H-β sample and on the 10Pd/active carbon reference sample.

RESULTS AND DISCUSSION

The Pt and Pd photolines are clearly visible in the XPS spectra of 3.0Pt0.5Pd/H-β, 1.5Pt0.25Pd/H-β, and the physical mixture of 1.5Pt/H-β and 0.25Pd/H-β (Figs. 1a–1c). The Pt 4*d* doublet at 332 eV ($4d_{3/2}$, peak 6) and 315 eV ($4d_{5/2}$,

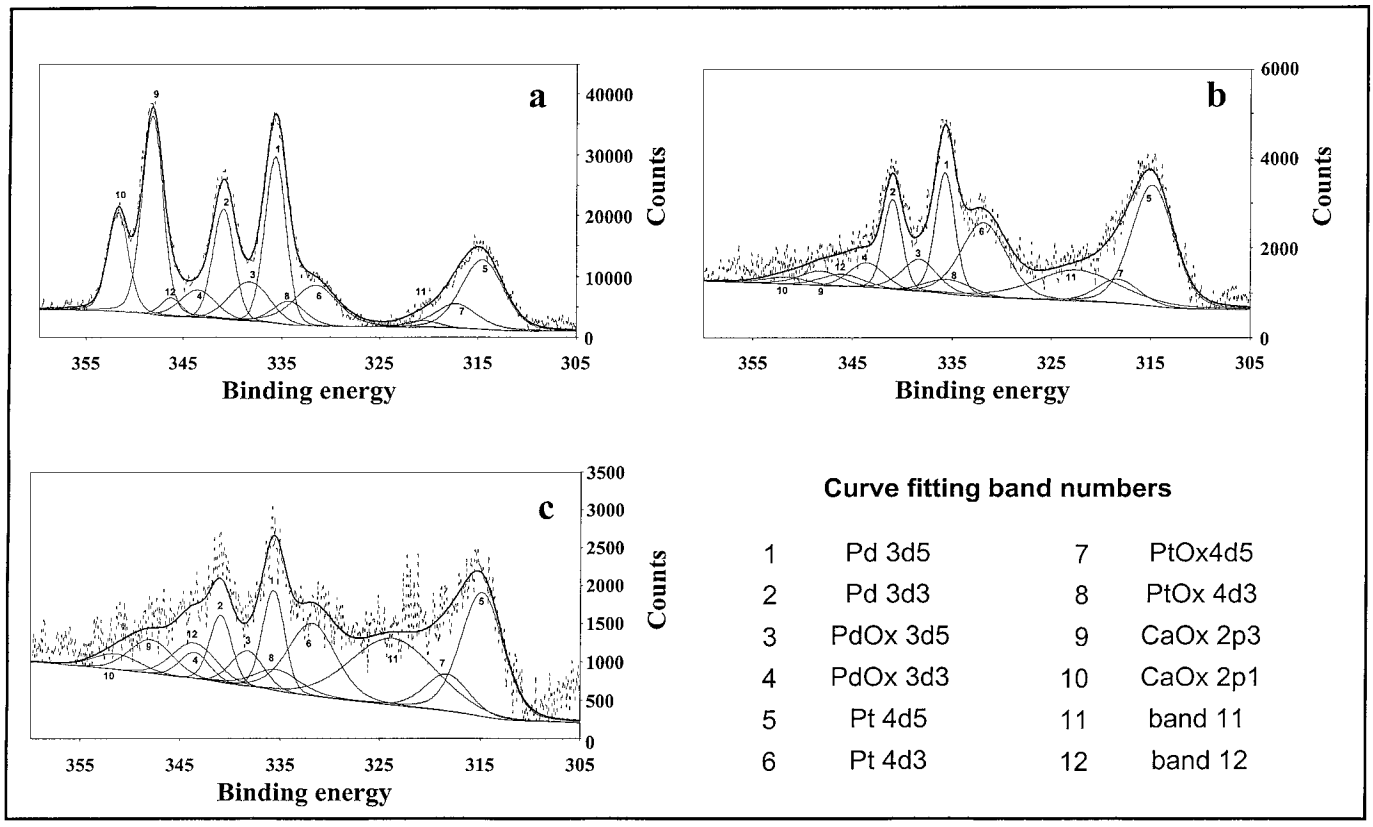

FIG. 1. XPS spectra in the Pt 4*d* and Pd 3*d* range before Ar^+ bombardment: (a) 3.0Pt0.5Pd/H-β; (b) 1.5Pt0.25Pd/H-β; (c) 1.5Pt/H-β + 0.25Pd/H-β physical mixture. Bands 11 and 12 are added as supplementary background subtraction.

peak 5) and the Pd 3*d* doublet at 335 eV ($3d_{5/2}$, peak 1) and 340 eV ($3d_{3/2}$, peak 2) are resolved with the expected intensity ratio of 1.5. Signals of electron-deficient Pt and Pd are also present (peaks 3, 4, 7, and 8). The XPS spectra recorded after sputtering with argon cations (Fig. 2) contain the same Pt 4*d* and Pd 3*d* doublets of metallic and electron-deficient Pt and Pd.

The XPS spectra in the Pt 4*f*, Al 2*p* region of the three samples before and after Ar^+ bombardment are shown in Figs. 3 and 4, respectively. These spectra were fitted with six components assigned to aluminum and platinum under reduced and oxidized form.

The Pt : Pd, Al : Pt, Al : Pd and Al : Pt + Pd atomic ratios in the three samples before and after argon cation bombardment, derived from the peak areas in Figs. 1–4 are reported in Table 3. In the 3.0Pt0.5Pd/H-β and 1.5Pt0.25Pd/H-β bimetallic catalysts before argon bombardment, the Pt : Pd atomic ratio is 1.2 and 2.4, respectively, which is lower than that according to the chemical composition, viz., 3 : 1. The sputtering operation leads to a significant increase of the platinum concentration relative to palladium and Pt : Pd atomic ratios higher than 3 : 1, viz., 4.4 and 3.2, respectively. In the physical mixture of Pt and Pd monometallic catalysts, the sputtering operation did not significantly alter the Pt : Pd atomic ratio. The sputtering yield of Pt and Pd in the Ar^+ energy range of 2500 eV are not expected to be very different. At 2 keV, the yields are 3.04 for palladium and 2.43 for platinum, the difference becoming smaller with increasing energy (15) so that preferential sputtering cannot explain our observations. If there were pronounced preferential palladium sputtering, the Pt : Pd ratio should also have changed in the physical mixture, which it did not. Considering that the sputtering removes a limited number of atomic layers, these changes are explained by the preferential removal of a palladium-rich rim of bimetallic particles with Pt-rich cores.

TABLE 3

Atomic Ratios before and after Ar^+ Bombardment

Atomic ratio	3.0Pt0.5Pd/H-β		1.5Pt0.25Pd/H-β		1.5Pt/H-β + 0.25Pd/H-β physical mixture	
	Before	After	Before	After	Before	After
Pt : Pd	1.2	4.4	2.4	3.2	3.0	2.8
Al : Pd	21	93	50	146	144	117
Al : Pt	17	21	21	46	48	43
Al : (Pt + Pd)	9.4	17	15	35	38	31

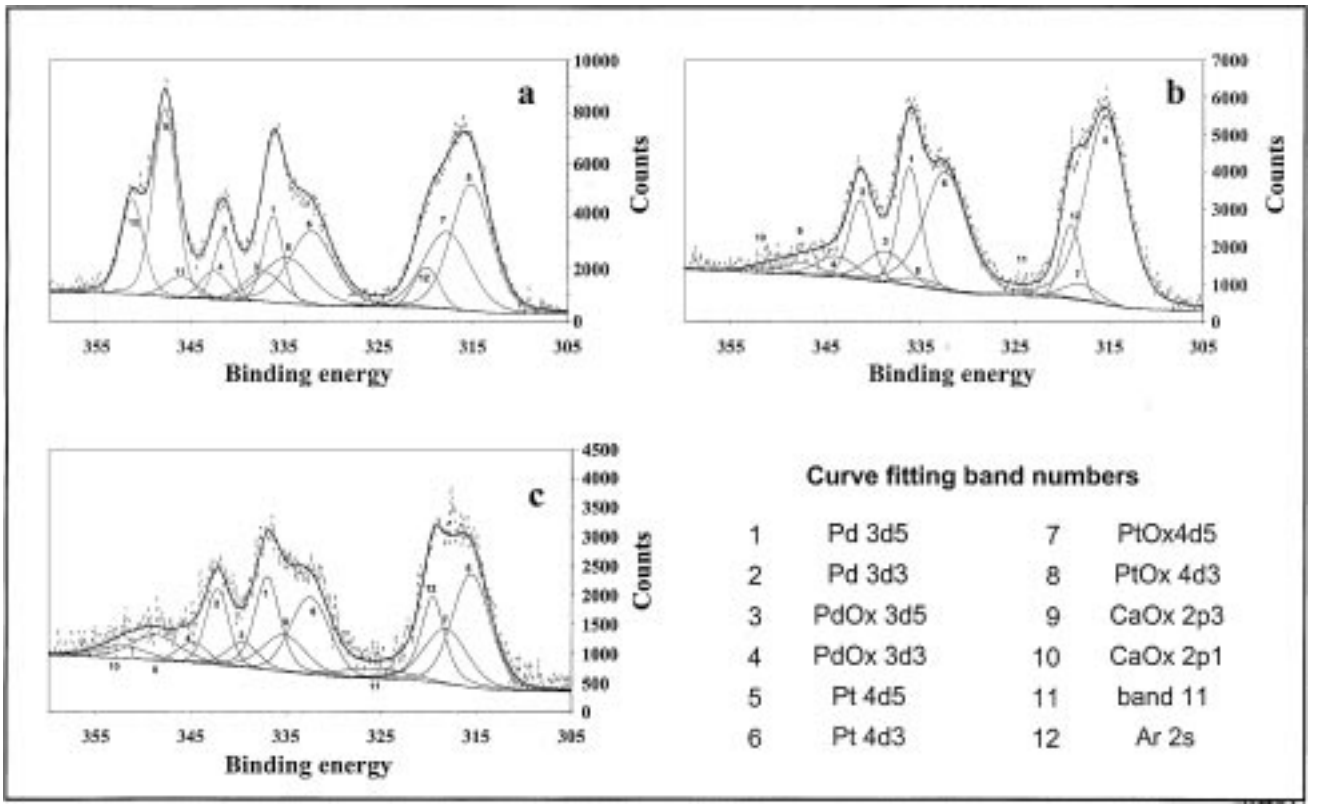

FIG. 2. XPS spectra in the Pt 4*d* and Pd 3*d* range after Ar^+ bombardment: (a) 3.0Pt0.5Pd/H-β; (b) 1.5Pt0.25Pd/H-β; (c) 1.5Pt/H-β + 0.25Pd/H-β physical mixture.

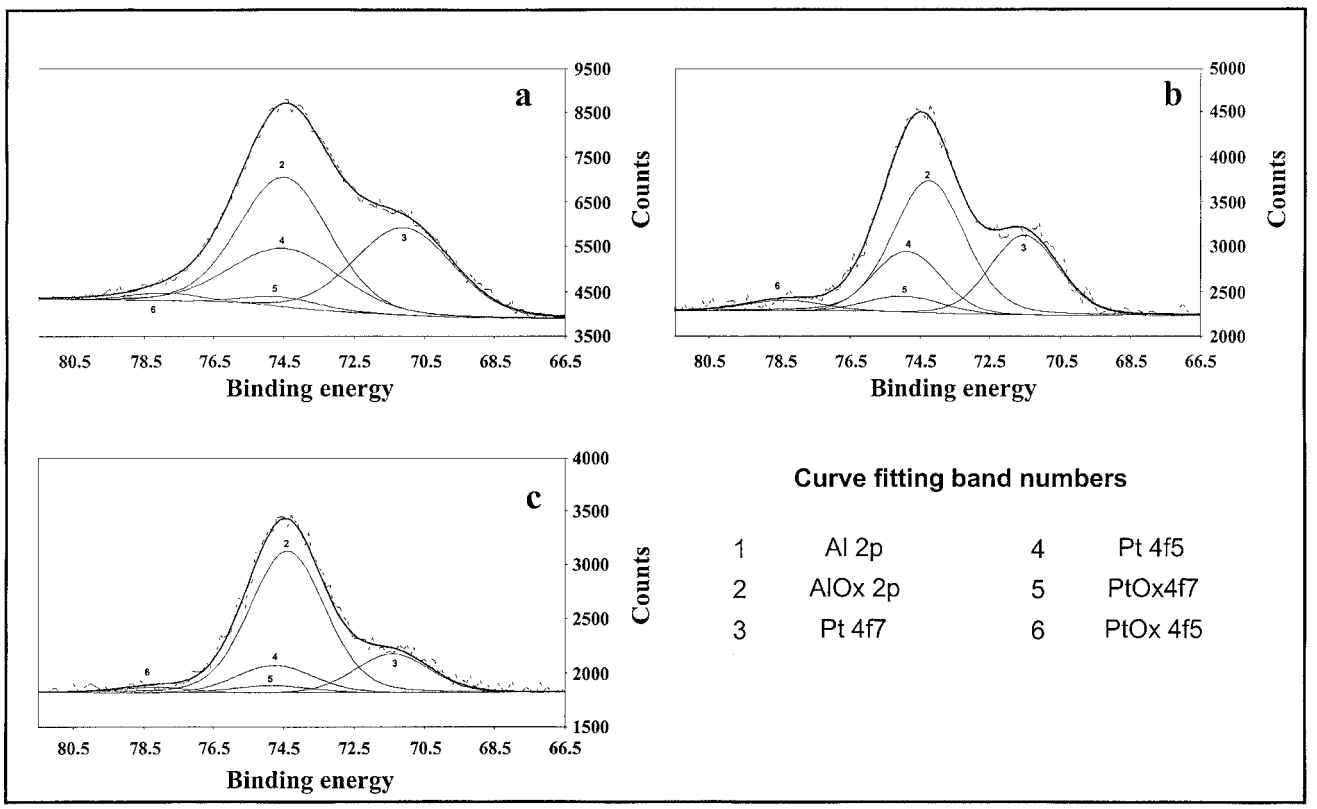

FIG. 3. XPS spectra in the Pt 4*f* and Al 2*p* range before Ar^+ bombardment: (a) 3.0Pt0.5Pd/H-β; (b) 1.5Pt0.25Pd/H-β; (c) 1.5Pt/H-β + 0.25Pd/H-β physical mixture.

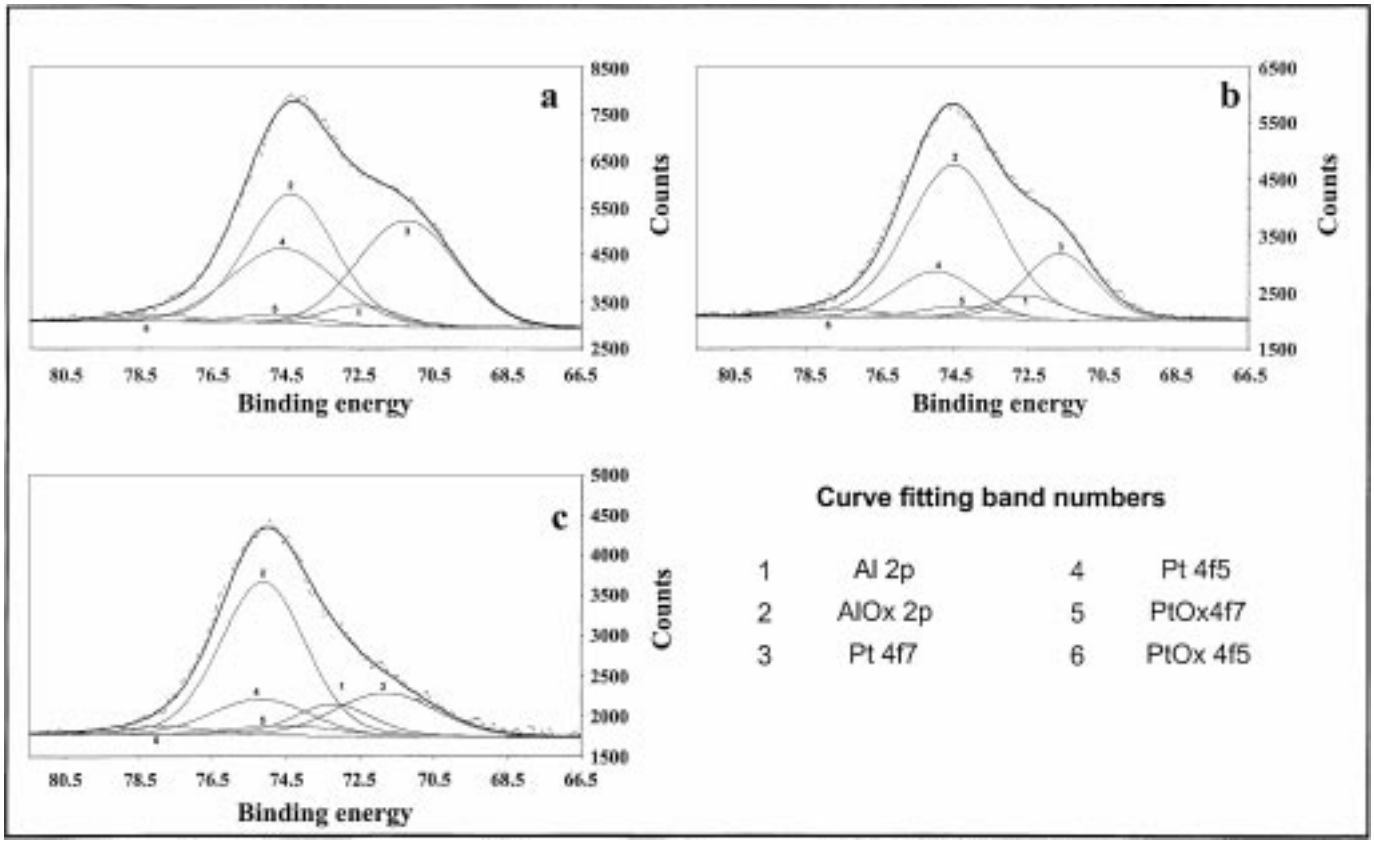

FIG. 4. XPS spectra in the Pt 4*f* and Al 2*p* range after Ar^+ bombardment: (a) 3.0Pt0.5Pd/H-β; (b) 1.5Pt0.25Pd/H-β; (c) 1.5Pt/H-β + 0.25Pd/H-β physical mixture.

In the bimetallic catalysts, the Al : Pt, Al : Pd, and Al : (Pt + Pd) ratios increased after the sputtering, while such an effect was not observed with the physical mixture of the monometallic catalysts. This is probably a particle size effect and can be explained by easier removal of the small Pt–Pd particles in the bimetallic catalysts, compared to the larger metal particles in the physical mixture.

The Pd $3d_{5/2}$/Pd_{MNN} intensity ratio measured as the surface area of the peaks and not normalized for particle size was 2.7 for a reference sample with large Pd particles (10 Pd/active carbon) compared to 1.9 on 3.0Pt0.5Pd/H-β. According to Venezia *et al.* (12), such a lower ratio is another indication of the presence of Pt–Pd bimetallic particles with Pd segregation to the surface in the 3.0Pt0.5Pd/H-β sample.

Palladium segregation to the surface of small Pt–Pd bimetallic particles supported on H-β zeolite presently revealed with XPS and argon cation bombardment was previously reported for other types of samples and derived from other types of measurements. Hansen *et al.* (14) used TEM, EXAFS, and segregation profile predictions based on *ab initio* orbital calculations and arrived at a similar palladium segregation model for their bimetallic Pt–Pd particles in dealuminated H-Y zeolites. Their catalysts had metal loadings similar to those in the present study, but lower Pt : Pd ratios from 1 : 3 to 1 : 1 compared to 3 : 1 in the present study. The formation of a platinum core structure was also found in the basic Na-Y zeolite, with a pronounced Pt core structure at a Pt : Pd ratio of 3 : 1 (13). Based on the present work on yet another zeolite type, the formation of bimetallic particles with a Pt-enriched core and a Pd-enriched surface was now also observed in H-β zeolites when using tetraamine precursors, high-temperature calcination, and hydrogen reduction for the catalyst preparation. The observation of a different behavior of Pt–Pd alloy particles in a pumice-supported catalyst with the less abundant metal segregated to the surface (12) could be due to the special metal deposition technique used involving anchoring of allyl derivatives on the support surface and hydrogen reduction at −10°C.

CONCLUSIONS

In bimetallic PdPt/H-β zeolite catalysts with a Pt : Pd atomic ratio of 3 : 1, prepared by impregnation of tetraamine metal complexes on H-β or cation exchange on NH_4-β, calcination, and reduction at 400°C, palladium segregation to the surface of bimetallic particles was revealed with XPS in combination with argon cation sputtering. The nature of the Pt–Pd bimetallic particles in PtPd/H-β

zeolites and PtPd/Y-type zeolites previously studied with other techniques seems to be similar.

ACKNOWLEDGMENT

This work was carried out in the frame of the IUAP-PAI collaborative research project, sponsored by the Belgian Federal government.

REFERENCES

1. Sinfelt, J. H., Via, G. H., and Lyttle, F. W., *Catal. Rev.-Sci. Eng.* **26**, 81 (1984).
2. Lin, T.-B., Jan, C.-A., and Chang, J.-R., *Ind. Eng. Chem. Res.* **34**, 4284 (1995).
3. Reinhoudt, H. R., Troost, R., van Langeveld, A. D., van Veen, J. A. R., Sie, S. T., and Moulijn, J. A., *Stud. Surf. Sci. Catal.* **127**, 251 (1999).
4. Lee, J.-K., and Rhee, H.-K., *J. Catal.* **177**, 208 (1998).
5. Martens, J. A., Perez-Pariente, J., and Jacobs, P. A., *Acta Phys. Chem. Szeged.* **31**, 487 (1985).
6. Smirniotis, P. G., and Ruckenstein, E., *J. Catal.* **140**, 526 (1993).
7. Blomsma, E., Martens, J. A., and Jacobs, P. A., *J. Catal.* **155**, 141 (1995); *J. Catal.* **159**, 323 (1996).
8. Blomsma, E., Martens, J. A., and Jacobs, P. A., *Stud. Surf. Sci. Catal.* **105**, 909 (1997).
9. Blomsma, E., Martens, J. A., and Jacobs, P. A., *J. Catal.* **165**, 241 (1997).
10. Carturan, G., Cocco, G., Facchin, G., and Navazio, G., *J. Mol. Catal.* **26**, 375 (1984).
11. Deganello, G., Duca, D., Liotta, L. F., Martorana, A., Venezia, A. M., Benedetti, A., and Fagherazzi, G., *J. Catal.* **151**, 125 (1995).
12. Venezia, A. M., Duca, D., Floriano, M. A., and Deganello, G., *Surf. Interface Anal.* **19**, 543 (1992).
13. Rades, T., Pak, C., Polisset-Thfoin, M., Ryoo, R., and Fraissard, J., *Catal. Lett.* **29**, 91 (1994).
14. Hansen, P. L., Molenbroek, A. M., and Ruban, A. V., *J. Phys. Chem. B* **101**, 1861 (1997).
15. Chambers, G. P., and Fine, J., *in* "Practical Surface Analysis" (D. Briggs and M. P. Seah, Eds.), Vol. 2, p. 705. Ion and Neutral Spectroscopy, Wiley, Chichester, New York, 1992.
16. Bearden, J. A., and Burr, A. F., *Rev. Mod. Phys.* **39**, 125 (1967).